

## Spin-resolved substrate band mapping in Fe/Cu(100): Application of the spin-filter effect

W. Kuch, M.-T. Lin, K. Meinel, and C. M. Schneider

*Max-Planck-Institut für Mikrostrukturphysik, Weinberg 2, D-06120 Halle, Germany*

J. Noffke

*Institut für Theoretische Physik, Technische Universität Clausthal,  
D-38678 Clausthal-Zellerfeld, Germany*

J. Kirschner

*Max-Planck-Institut für Mikrostrukturphysik, Weinberg 2, D-06120 Halle, Germany*

(Received 23 September 1994)

Spin-oriented, normally emitted Cu 3*d* photoelectrons, generated by circularly polarized synchrotron radiation in the energy range of 10–24 eV, are transmitted through perpendicularly magnetized ultrathin fcc iron films on Cu(100). Spin-dependent scattering of electrons of majority and minority spin with respect to the Fe magnetization direction results in an intensity asymmetry, which is 22% for electrons with kinetic energies of 5 eV and an Fe film thickness of 4.3 monolayers. Exploiting this effect, the iron film is used as a very efficient spin detector to investigate spin-dependently the relativistic bulk band structure of the Cu 3*d* states in Fe/Cu(100). Good agreement with fully relativistic band-structure calculations is found.

### I. INTRODUCTION

Spin-dependent scattering events are an important mechanism leading to the spin polarization of secondary electrons in ferromagnets. Spin dependent transmission of electrons through ferromagnetic overlayers has been reported by Pappas *et al.*<sup>1</sup> for fcc iron on Cu(100) and more recently by Getzlaff, Bansmann, and Schönhense for thin iron and cobalt films on W(110).<sup>2</sup> They observed a spin polarization of the formerly unpolarized substrate photoemission signal after transmission through a ferromagnetic overlayer. Electrons with a spin direction representing majority electrons with respect to the magnetization direction of the ferromagnet are less attenuated by scattering events than those representing minority electrons. The magnitude of this transmission asymmetry, which for Fe/Cu(100) is on the order of 20%,<sup>1</sup> supports the idea of an application of thin magnetic films as highly efficient spin detectors.<sup>3</sup>

In this contribution we show how a thin fcc iron film, grown epitaxially on Cu(100), can be applied as a spin filter for the spin- and energy-resolved analysis of photoelectrons from the substrate crystal. Combining circularly polarized UV light with a conventional spin-integrating electron energy analyzer it is possible to study spin dependently the dispersion of the spin-orbit split substrate bands by solely measuring spin-integrated photoelectron spectra. The Fe film thereby acts as a spin detector with a high figure of merit of approximately  $4 \times 10^{-3}$ .

Spin-resolved photoemission experiments have the advantage that the relativistic band structure, including the

effect of spin-orbit coupling, is directly accessible, even if this effect should be small. The influence of the spin-orbit interaction on the electronic structure, however, has proved to be important even for low-*Z* materials such as Cu.<sup>4</sup> For normally emitted photoelectrons from the (100) plane of a fcc crystal and excitation with circularly polarized radiation, relativistic selection rules allow only transitions from states exhibiting  $\Delta_6^5$  or  $\Delta_7^5$  symmetry into the  $\Delta_6^1$  final band.<sup>5</sup> For excitation with circularly polarized light of normal incidence, these transitions show an optical spin orientation normal to the crystal surface. Measuring this spin polarization component permits the connection of the experimental data with fully relativistic band-structure calculations.

Spin-polarized electrons from the copper substrate with their spin parallel and antiparallel to the surface normal represent electrons of majority and minority type in the perpendicularly magnetized iron film. Different scattering for both spin orientations in this film can result in a difference of the measured intensity. At the clean Cu sample, reversing the light helicity reverses the spin directions of the  $\Delta_6^5$  and  $\Delta_7^5$  emission features, but does not lead to an asymmetry in spin-integrated photoemission intensity. If the same photoelectrons have to pass through a thin film in which electrons of different spin orientations undergo a different attenuation, a reversal of the light helicity, which means a reversal of the spin directions, would produce different intensity spectra. Hence, spin polarization in the substrate photoemission signal can be detected as an intensity asymmetry after transmission through a magnetic overlayer, given a spin-dependent scattering in the overlayer. For

incident light of positive (negative) helicity, transitions from states with  $\Delta_8^5$  symmetry into the final state band of  $\Delta_6^1$  symmetry are allowed only for electrons with the spin antiparallel (parallel) to the surface normal.<sup>5</sup> Transitions from states with  $\Delta_7^5$  symmetry are allowed only for electrons with the opposite spin direction. If majority electrons are less attenuated, spectral features originating from  $\Delta_7^5$  states would thus show a higher intensity if the magnetization direction and the vector of the light helicity are aligned antiparallel, and a lower intensity for parallel alignment.

For the detection of the spin polarization perpendicular to the surface using a thin magnetic film as a spin detector, the system Fe/Cu(100) is well suited. First, it shows a strong uniaxial magnetic anisotropy normal to the surface; second, the epitaxial growth of iron on Cu(100) as well as the structural and magnetic properties have been studied extensively and are the topic of numerous publications.<sup>6–17</sup> At room temperature, iron grows on a Cu(100) surface up to a thickness of ten monolayers (ML) epitaxially in a layer-by-layer fashion, forming a pseudomorphic film of fcc iron.<sup>6–8</sup> Although there seems to be some inconsistency in the literature, the easy axis of the magnetization of these films is perpendicular to the surface up to a film thickness of at least 6 ML.<sup>7,9–13</sup>

## II. EXPERIMENT

Iron films were deposited from an iron rod of 99.99% purity via electron bombardment with the sample held at 120 K and subsequent annealing at 300 K, following the procedure proposed in Ref. 14. These films showed no deviation in their properties presented in this paper compared to films deposited at room temperature. Typical deposition rates were 1 ML/min, while the overall pressure rise in the vacuum chamber did not exceed  $4 \times 10^{-8}$  Pa. No surface contamination above the Auger detection limit ( $\approx 1\%$ ) could be detected after iron deposition. Photoemission spectra were taken at the 6.5-m normal-incidence monochromator beam line of the Berlin synchrotron radiation facility (BESSY), which offers a degree of circular polarization of about 90%.<sup>18</sup>

To ensure the full power of the above mentioned selection rules and to rule out spin-dependent transmission-induced asymmetries at the Fe/Cu interface,<sup>19</sup> all spectra presented in this paper were taken in the totally symmetric configuration, i.e., normal incidence of the incoming radiation and normal emission of the outgoing photoelectrons. The magnetization direction of the Fe films was perpendicular to the surface, being thus aligned with both photon and photoelectron wave vectors.

The spectrometer used is described in detail elsewhere.<sup>4</sup> In brief, it consists of a  $60^\circ$  segment of a cylindrical mirror analyzer with an input lens system and a virtual input aperture. This system allows the detection of normally emitted electrons for normal incidence of the incoming light. It was operated at a fixed pass energy of 8 eV, resulting in an energetic overall resolution of 180 meV with the monochromator set to a photon energy of 12 eV. The electrons passing through the exit

slit of the analyzer are either electrostatically reflected or diffracted at a W(100) surface for the measurement of spin-integrated or spin-resolved spectra, respectively, and then detected via a two-stage channel plate.

The iron films were magnetized *in-situ* with perpendicular remanence. The magnetization was checked before and after the photoemission experiments by means of polar magneto-optic Kerr-effect measurements. All films exhibited the known rectangular hysteresis loops.<sup>10</sup> The magnetization procedure as well as the photoemission measurements were performed at a sample temperature of 150 K. This temperature was chosen to be, on the one hand, well below the Curie temperature of the film. On the other hand, it had to be high enough to ensure that the maximum field of the available magnetization coil of approximately 200 Oe is exceeding well the saturation field of the Fe film.

Spectra for both helicities of the incoming light were taken for both magnetization directions to rule out apparatus induced asymmetries.

## III. RESULTS AND DISCUSSION

In the topmost panel of Fig. 1, photoemission spectra for 4.3 ML Fe on Cu(100) are shown on the left-hand side [Fig. 1(a)] for the vectors of the light helicity and the film magnetization parallel [ $I(\uparrow\uparrow)$ , dashed line] and antiparallel [ $I(\uparrow\downarrow)$ , dotted line] as well as the sum of both (solid line). Also shown is a Shirley-type background, which we will discuss later. On the right-hand side [Fig. 1(b)], the normalized asymmetry  $A$  is depicted, defined as  $A = [I(\uparrow\downarrow) - I(\uparrow\uparrow)]/[I(\uparrow\downarrow) + I(\uparrow\uparrow)]$ . The peak around 2.2 eV binding energy can be attributed to an emission from the 3d states of Cu(100).<sup>4</sup> It shows a clearly visible peak-to-peak asymmetry of 5.5% upon changing either the sign of the light helicity or the magnetization direction. The asymmetry at lower binding energies originates from magnetic circular dichroism of Fe 3d states and will be discussed in a forthcoming publication.

Reference photoemission spectra of the clean Cu(100) surface at the same photon energy of 12 eV, which are measured in the spin-resolved mode of the electron analyzer, are reproduced in the bottom of Fig. 1. Similar to panel (a), spectra with the vectors of the photoelectron spin and the light helicity parallel and antiparallel are reproduced in Fig. 1(g) with a dashed and dotted line, respectively. The solid line is the spin-integrated intensity. On the right-hand side [Fig. 1(h)] the respective spin polarization, defined in analogy to the asymmetry  $A$  and corrected for the detector spin sensitivity, is depicted.

The shape of the intensity asymmetry spectrum of Fe/Cu(100) in the Cu 3d region [Fig. 1(b)] resembles strongly the spin polarization of the Cu 3d photoelectrons from the clean sample [Fig. 1(h)], which reaches values of +45% and -25%. This spin orientation perpendicular to the crystal surface in emission from a paramagnet is a consequence of the spin-orbit interaction, which causes a coupling of the spatial and spin parts of the transition matrix elements, and is governed by relativistic selection rules. The contribution at 2.3 eV binding energy orig-

inates from a transition from an initial band with  $\Delta_6^5$  double group representation to a  $\Delta_6^1$  final band, whereas the contribution at 2.1 eV binding energy results from a transition from a  $\Delta_7^5$  band into the  $\Delta_6^1$  band. The strong resemblance of the spin polarization of Cu(100) and the intensity asymmetry of Fe/Cu(100) leads to the conclusion that the origin of the observed asymmetry is indeed the spin polarization of the substrate photoemission signal. The  $\Delta_7^5$  emission shows higher intensity for antiparallel alignment of the magnetization direction and the vector of the light helicity. As already pointed out, this is expected for spin-dependent scattering of the elec-

trons in the magnetic film, if electrons of majority spin are less attenuated.

To quantify this effect, the spectra of Fig. 1(b) and Fig. 1(h) have to be compared. Therefore, in a first step, the Fe-induced background in the Cu 3d region has to be subtracted. Doing this with a Shirley-type background as indicated in Fig. 1(a) results in the spectra shown in Fig. 1(c). Again, the resulting intensity spectra for parallel and antiparallel alignment of the magnetization and the light helicity as well as the sum of both are reproduced. The accompanying asymmetry spectrum is shown in Fig. 1(d). To enable a quantitative comparison of these spectra with the spectra from pure Cu(100), the starting point of the Shirley iterations and the slope of the background were chosen in such a way that the remaining Cu 3d spectra [Fig. 1(c)] have the same background/intensity ratio as the spectra of Fig. 1(g). The exact shape of the background is not crucial for the result of the quantification, which was checked by trying different types of background.

Comparing Figs. 1(d) and 1(h), a very good similarity of the curves can be seen. The intensity asymmetry of Fig. 1(d) amounts to 22% of the spin polarization of Fig. 1(h), which means that the spin sensitivity of the Fe film is  $S = 0.22$ . Scaling the asymmetry of Fig. 1(d) by  $1/S$  results in the spectrum of Fig. 1(f), which is nearly the same as the spin polarization spectrum of Fig. 1(h). Using the scaled asymmetry spectrum of Fig. 1(f) and the total intensity spectrum [solid line of Fig. 1(c)], corresponding partial intensities can be calculated. They are shown together with the total intensity in Fig. 1(e). Like the asymmetry, they also show a strong resemblance to the spin-resolved measurement of Cu(100) [Fig. 1(g)]. Slight differences in the relative height of the partial intensities can be attributed to the somewhat arbitrary background removal procedure. To summarize, taking a pair of intensity spectra acquired with circularly polarized light of opposite helicity and performing the above procedure, i.e., subtraction of the inelastic background of the Fe 3d emission at the Cu 3d region and subsequent scaling of the intensity asymmetry by  $1/S$ , hence results in spin-resolved spectra of the substrate. The observed intensity asymmetry is thus traced back to its origin, the spin polarization caused in the Cu(100) substrate by circularly polarized light. The Fe film acts as a spin filter, which may be used to obtain spin-resolved substrate photoemission spectra [Fig. 1(e)].

For the quantification of the spin-filter effect one has to recall the value of  $S = 0.22$ . This means that a 100% spin-polarized input signal causes an intensity asymmetry of 22%. A spin filter consisting of a 4.3-ML Fe film on Cu(100) has thus a spin-filter efficiency of 22% for transmitted electrons of 5 eV kinetic energy. This value is slightly higher than the one obtained by Pappas *et al.* for a similar electron kinetic energy and film thickness<sup>1</sup> and also slightly higher than the theoretically obtained value of Gokhale and Mills, assuming purely elastic scattering as mechanism for the spin asymmetry.<sup>20</sup> To obtain the figure of merit  $S^2T$  of the spin filter applied as a spin polarizer, the transmittivity  $T$  of the film must also be determined. Assuming an inelastic mean free path of 5

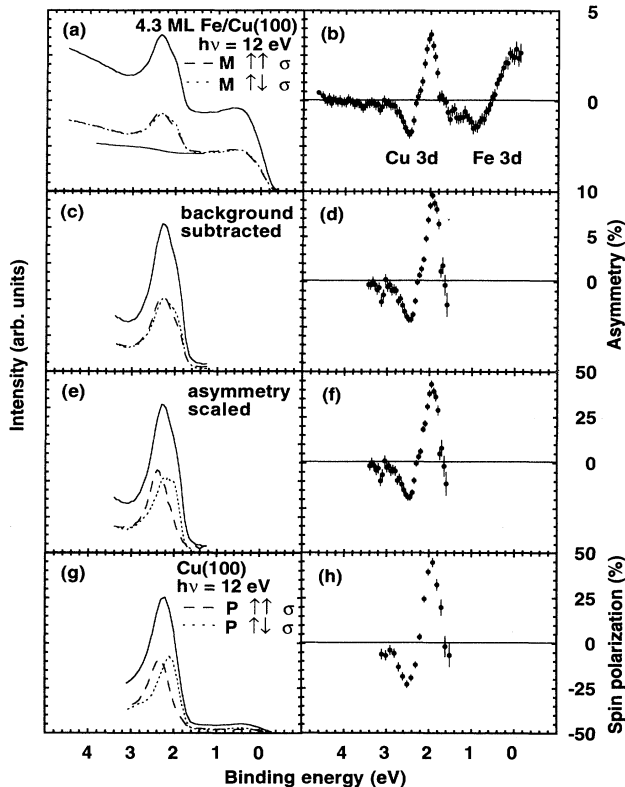


FIG. 1. (a) Photoelectron spectra of 4.3 ML Fe/Cu(100) at 12 eV photon energy for the direction of the film magnetization  $M$  parallel (dashed line) and antiparallel (dotted line) to the helicity  $\sigma$  of the exciting light, as well as the sum of both (solid line). (b) Asymmetry  $A$ , calculated from the spectra of (a) using the formula  $A = [I(\uparrow\downarrow) - I(\uparrow\uparrow)]/[I(\uparrow\downarrow) + I(\uparrow\uparrow)]$ . (c) Same as (a), but in the region of the Cu 3d peak corrected for the background induced by the Fe 3d emission as indicated in (a). (d) Asymmetry, calculated from the spectra of (c). (e) Total intensity curve (solid line) identical to the one in (c), partial intensities calculated from an asymmetry which is scaled by  $1/S$  ( $S = 0.22$ , spin-filter efficiency) with respect to the one shown in (d). (f) Asymmetry corresponding to the spectra of (e). (g) Spin-resolved photoelectron spectra of clean Cu(100) at 12 eV photon energy. Given are the spectra for the vectors of the electron spin polarization  $P$  and the light helicity  $\sigma$  parallel (dashed line) and antiparallel (dotted line) as well as the spin integrated spectrum (solid line). (h) Spin polarization  $P$ , calculated from the spectra of (g) using the formula  $P = [I(\uparrow\downarrow) - I(\uparrow\uparrow)]/[I(\uparrow\downarrow) + I(\uparrow\uparrow)]$ .

Å for the photoelectrons in the Fe film<sup>1</sup> results in an attenuation by a factor of 5 for the copper photoemission signal. Furthermore, the contribution of the iron-induced background to the statistics of the Cu 3*d* signal has to be taken into account. The respective signal-to-noise ratio can be estimated from Fig. 1(a) to be 1:1.2 at the Cu 3*d* peak energy. This yields an additional factor of 0.45 for *T*, ending up with a value of *T* = 0.09. Thus a figure of merit of approximately  $4 \times 10^{-3}$  is reached. While this value is higher than that of most of the conventional spin detectors, the main advantage of this spin filter is that no external spin detector is required for the acquisition of spin-resolved substrate photoemission spectra. It is therefore straightforward to use the spin filter as a polarizer for the spin-dependent observation of copper substrate valence states.

A determination of spin-resolved peak positions can be made after correction of the spin-filter efficiency. The value obtained by comparison with spin-resolved measurements at 12 eV photon energy, namely, 0.22, is assumed for all photon energies up to 24 eV. This may not be fully adequate, especially for higher photon energies, since the measurements of Pappas *et al.*<sup>1</sup> indicate a reduction of the spin-filter efficiency at higher kinetic energies of the transmitted electrons. The obtained spin polarization at higher photon energies may therefore underestimate the real value as it would be obtained at the pure Cu(100) surface. The peak positions determined from spectra corrected by a spin sensitivity of 0.22, however, do not differ from those obtained from spectra which are corrected by different spin sensitivities within a factor of 2.

A series of partial intensity spectra for different photon energies corrected with the constant value of 0.22 is shown in Fig. 2. Here, in contrast to Fig. 1(e), the iron-induced background has not been subtracted. Subtraction of the background before or after correction for the spin sensitivity makes only a negligible difference in the determined peak positions. They are indicated in Fig. 2 by open and solid symbols according to the symmetry of the initial state bands. Peaks in the partial intensity curves for antiparallel alignment of the magnetization direction and the photon helicity (dotted lines in Fig. 2) belong to an initial state band of  $\Delta_7^5$  symmetry and are marked by open triangles. Peaks obtained for parallel alignment (solid lines in Fig. 2) correspond to  $\Delta_6^5$  symmetry and are marked by solid triangles. The Cu 3*d* peak shows a distinct dispersion towards higher binding energies with increasing photon energy. At the same time the peak width increases. This is partially due to the worse resolution of the light monochromator at higher photon energies, which results in an overall resolution of approximately 300 meV for  $h\nu = 24$  eV. An additional contribution to the broadening of the Cu 3*d* peak comes from the shoulder in the partial spectra for  $\Delta_6^5$  symmetry at  $h\nu = 21$  eV and  $h\nu = 24$  eV at 3.2 eV binding energy.

In Fig. 3, the peak positions are plotted as solid squares versus the momentum vector *k* along the  $\Delta$  axis. Peak positions attributed to  $\Delta_6^5$  and  $\Delta_7^5$  states are reproduced in the left- and right-hand panels, respectively. The *k*

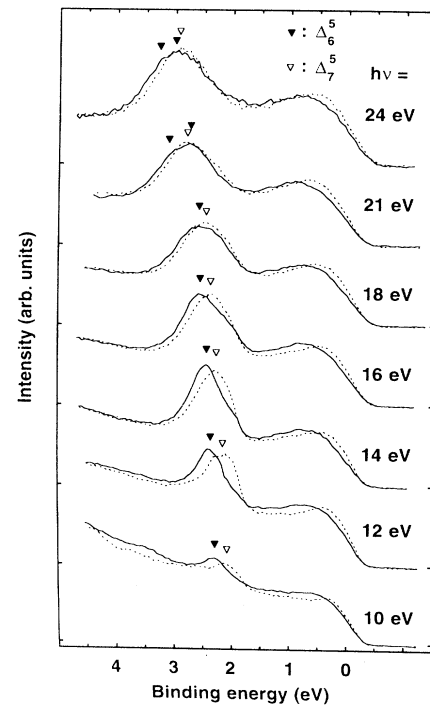


FIG. 2. Series of partial intensity spectra for different photon energies  $h\nu$ . Shown are spectra for the direction of the film magnetization and the light helicity parallel (solid lines) and antiparallel (dotted lines), calculated from the respective total intensity curves using an asymmetry corrected for the spin-filter efficiency of 0.22. Peak positions due to transitions from initial state bands containing  $\Delta_6^5$  or  $\Delta_7^5$  symmetry are indicated by solid and open triangles, respectively.

values were determined taking the  $\Delta_6^1$  final state band for copper from the calculation of Eckhardt, Fritsche, and Noffke.<sup>21</sup> It is *a priori* not clear that final state bands of copper are the correct choice when using the three-step model of photoemission in that particular case. The main contribution to the detected Cu 3*d* photoemission signal originates from copper atoms near the Fe/Cu interface, and it is conceivable that due to hybridization effects between iron and copper final state bands the *k* values obtained from pure copper band-structure calculations may be somewhat wrong. The use of free-electron final states and the variation of the inner potential in a reasonable range, however, provided no indication of other than copper final state bands involved in the transitions.

The relativistic band structure calculated by Eckhardt, Fritsche, and Noffke<sup>21</sup> is reproduced in Fig. 3 as dotted lines together with the experimental peak positions. Bands with  $\Delta_6^5$  and  $\Delta_7^5$  symmetry are given in the left- and right-hand panels, respectively. Due to hybridization with bands of  $\Delta_6^1$  and  $\Delta_7^2$  symmetry, for which no transitions to the  $\Delta_6^1$  final state band are allowed,<sup>5</sup> there are in each case two bands containing portions of  $\Delta_6^5$  and  $\Delta_7^5$  symmetry. The amount of  $\Delta_6^5$  or  $\Delta_7^5$  symmetry, which was obtained from linear augmented plane wave (LAPW) calculations, is indicated in Fig. 3 by the density of the dotted lines. In the right-hand panel, for ex-

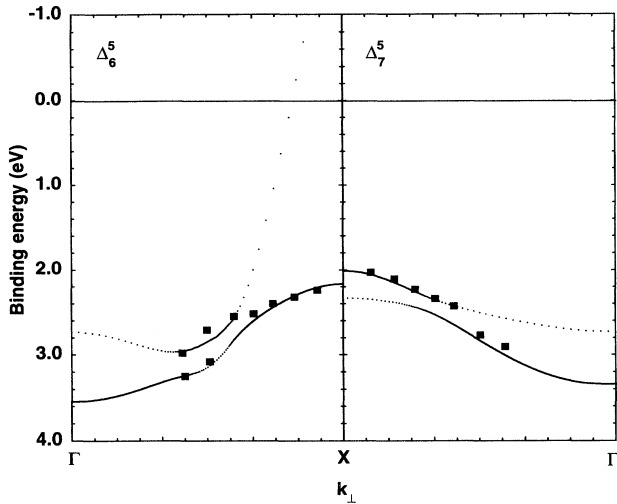


FIG. 3. Relativistically calculated band structure of copper along the  $\Delta$  axis (dotted lines, from Ref. 21), together with the experimentally observed spin-resolved photoemission peaks from Fig. 2. Left: bands containing portions of  $\Delta_6^5$  symmetry and experimental peak positions for spin polarization parallel to the light helicity. Right: bands containing portions of  $\Delta_7^5$  symmetry and experimental peak positions for spin polarization antiparallel to the light helicity. The portions of  $\Delta_6^5$  and  $\Delta_7^5$  symmetry are indicated by the density of the dotted lines.

ample, the lower-lying band at the  $\Gamma$  point has pure  $\Delta_7^5$  symmetry, which on the way to the  $X$  point is changed by hybridization with the higher-lying band to give mainly  $\Delta_7^2$  symmetry at the  $X$  point.

Comparing the experimental spin-resolved data, obtained with a thin iron film as spin detector, with the relativistic band structure for Cu, very good agreement can be seen. The spin-orbit splitting at the  $X$  point is determined experimentally to be about 150 meV, in agreement with spin-resolved photoemission measurements at clean Cu(100).<sup>4</sup> The hybridization-induced change of symmetry character between different bands in the relativistic band structure is observed experimentally. For  $\Delta_6^5$  symmetry, an additional shoulder in the Cu  $3d$  peak towards higher binding energies shows up at  $h\nu = 21$  eV and  $h\nu = 24$  eV and may yet be present at  $h\nu = 18$  eV, but is not well resolved at that photon energy. This shoulder is, like all the  $\Delta_6^5$  emission features at smaller photon energies, due to transitions from the lower-lying band of  $\Delta_6^5$  symmetry, which shows a strong dispersion in the middle of the Brillouin zone. The main contribution to the  $\Delta_6^5$  spectra for photon energies higher than 18 eV originates from transitions from the higher-lying  $sp$ -like band and is allowed only because of hybridization with the other band. At  $h\nu = 18$  eV (third data point from the left in Fig. 3) the energetic separation between the two bands reaches a minimum, which may account for the fact that there is only one peak resolved in the respective photoemission spectrum. For  $\Delta_7^5$  symmetry a discontinuity in the dispersion of the photoemission peak towards higher

binding energies is observed between 18 eV and 21 eV photon energy. The peak position shifts from 2.4 eV binding energy at  $h\nu = 18$  eV to 2.8 eV at  $h\nu = 21$  eV. This corresponds to the exchange of  $\Delta_7^5$  symmetry character between the two bands shown in the right-hand panel of Fig. 3, when the electron momentum parallel to the surface normal becomes smaller.

So far, all of the observed photoemission features could be explained in terms of the relativistic copper bulk band structure. Apart from this appears a small shoulder around 1.9 eV binding energy in the  $\Delta_6^5$  partial spectra for 12, 14, and 16 eV photon energy, which has no counterpart in the copper bulk band structure. It may be explained as emission from interface states or as the result of a hybridization between iron and copper states. In spite of the fact that the photoemission signal from the Cu  $3d$  states originates to a great extent from a region near the iron/copper interface (30% from the first atomic Cu layer, assuming an inelastic mean free path of 5 Å), however, no major contributions of a hybridization with the iron bands or from the interface are observed.

For the spin-resolved observation of substrate photoemission via the spin-filter effect any magnetic overlayer may be used, provided that it has a remanent magnetization along the desired quantization axis. A necessary prerequisite will of course be that the surface be entirely covered by the film; otherwise the spin-filter effect will be diminished by unscattered photoelectrons from the substrate. Epitaxial layer-by-layer growth of the films is not necessarily required. Recent scanning tunneling microscopy (STM) investigations<sup>22</sup> have revealed that the morphology of iron films on Cu(100) depends strongly on the preparation conditions. Films deposited at 130 K and annealed to room temperature exhibit a modified Stranski-Krastanov growth mode rather than a layer-by-layer growth. We recall that no difference in the spin-filter properties between iron films grown at room temperature and films deposited at 130 K and subsequently annealed to room temperature was observed. Thus the spin-filter effect happens to be independent of the growth mode in that case. It remains to be seen how it is affected by structural and magnetic properties in other systems.

#### IV. CONCLUSION

We have shown that an epitaxial film of Fe on Cu(100) leads to an intensity asymmetry of normally transmitted spin-polarized Cu photoelectrons. This asymmetry amounts to 22% for entirely spin-polarized electrons of 5 eV kinetic energy and an Fe film thickness of 4.3 ML. Using circularly polarized light, the spin-polarized emission of photoelectrons from the Cu  $3d$  bands can be observed as intensity asymmetry upon reversing the light helicity or the film magnetization direction. It was demonstrated how such a spin filter can be applied as a spin analyzer. Doing this, the spin-dependent band structure of Cu was determined and compared to fully relativis-

tic band-structure calculations. The peaks in the Cu 3*d* region of the photoemission spectra are found to be predominantly due to transitions between bands of the copper bulk band structure. Good agreement between the experimental data and the calculated band structure can be stated.

#### ACKNOWLEDGMENTS

We like to thank B. Zada for technical assistance during the measurements at BESSY. Financial support by the German minister of science and technology (BMFT) under Grant No. 05 5EFAAI5 is gratefully acknowledged.

- 
- <sup>1</sup> D. P. Pappas, K.-P. Kämper, B. P. Miller, H. Hopster, D. E. Fowler, C. R. Brundle, A. C. Luntz, and Z.-X. Shen, *Phys. Rev. Lett.* **66**, 504 (1991).
- <sup>2</sup> M. Getzlaff, J. Bansmann, and G. Schönhense, *Solid State Commun.* **87**, 467 (1993).
- <sup>3</sup> G. Schönhense and H. C. Siegmann, *Ann. Phys. (Leipzig)* **2**, 465 (1993).
- <sup>4</sup> C. M. Schneider, J. J. de Miguel, P. Bressler, P. Schuster, R. Miranda, and J. Kirschner, *J. Electron Spectrosc. Relat. Phenom.* **51**, 263 (1990).
- <sup>5</sup> M. Wöhlecke and G. Borstel, *Phys. Rev. B* **23**, 980 (1981).
- <sup>6</sup> M. Wuttig and J. Thomassen, *Surf. Sci.* **282**, 237 (1993).
- <sup>7</sup> J. Thomassen, F. May, B. Feldmann, M. Wuttig, and H. Ibach, *Phys. Rev. Lett.* **69**, 3831 (1992).
- <sup>8</sup> J. Giergiel, J. Kirschner, J. Landgraf, J. Shen, and J. Woltersdorf, *Surf. Sci.* **310**, 1 (1994).
- <sup>9</sup> R. Allenspach and A. Bischof, *Phys. Rev. Lett.* **69**, 3385 (1992).
- <sup>10</sup> C. Liu, E. R. Moog, and S. D. Baader, *Phys. Rev. Lett.* **60**, 2422 (1988).
- <sup>11</sup> D. Pescia, M. Stampanoni, G. L. Bona, A. Vaterlaus, R. F. Willis, and F. Meier, *Phys. Rev. Lett.* **58**, 2126 (1987).
- <sup>12</sup> M. Stampanoni, *Appl. Phys. A* **49**, 449 (1989).
- <sup>13</sup> M. T. Kief and W. F. Egelhoff, Jr., *J. Appl. Phys.* **73**, 6195 (1993).
- <sup>14</sup> D. A. Steigerwald, I. Jacob, and W. F. Egelhoff, Jr., *Surf. Sci.* **202**, 472 (1988).
- <sup>15</sup> D. P. Pappas, K.-P. Kämper, B. P. Miller, H. Hopster, D. E. Fowler, A. C. Luntz, and C. R. Brundle, *J. Appl. Phys.* **69**, 5209 (1991).
- <sup>16</sup> P. Xhonneux and E. Courtens, *Phys. Rev. B* **46**, 556 (1992).
- <sup>17</sup> M. T. Kief and W. F. Egelhoff, Jr., *Phys. Rev. B* **47**, 10785 (1993).
- <sup>18</sup> F. Schäfers, W. Peatman, A. Eyers, C. Heckenkamp, G. Schönhense, and U. Heinzmann, *Rev. Sci. Instrum.* **57**, 1032 (1986).
- <sup>19</sup> H. P. Oepen, K. Hünlich, and J. Kirschner, *Phys. Rev. Lett.* **56**, 496 (1986).
- <sup>20</sup> M. P. Gokhale and D. L. Mills, *Phys. Rev. Lett.* **66**, 2251 (1991).
- <sup>21</sup> H. Eckardt, L. Fritsche, and J. Noffke, *J. Phys. F* **14**, 97 (1984).
- <sup>22</sup> J. Giergiel, J. Shen, J. Woltersdorf, A. Kirilyuk, and J. Kirschner (unpublished).